2015 IEEE International Conference on Robotics and Automation (ICRA)
Washington State Convention Center
Seattle, Washington, May 26-30, 2015

Robot-Inspired Biology: The Compound-Wave Control Template

Jin Dai[1], Matthew Travers[1], Tony Dear[1], Chaohui Gong[1], Henry C. Astley[2], Daniel I Goldman[2] and Howie Choset[1]

***Abstract*— Biologically inspired robots perform many interesting and useful behaviors, but to effectively emulate their biological counterparts, robots often need to possess many degrees of freedom, complicating their mechanical design and making it difficult to apply standard control and motion planning strategies. To address this complexity, the robotics community has derived low-dimensional parameter-based controllers that naturally coordinate many degrees of freedom such as the *serpenoid curves* used to control snake robots. Controllers utilizing this parameterization for snake robots have been able to induce behaviors similar to that of the robots' biological counterparts. A similar concept, called a *control template*, is used in the study of animal movements. However, much of the prior work on control templates has been limited to in-plane motion. In this work, we extend the usage of control templates to three dimensions to both better model and understand biology, as well as to help us gain better intuition into how we can use pre-existing control paradigms to create new behaviors for biologically inspired robots.**

I. INTRODUCTION

Snake robots exhibit many behaviors similar to biological snakes, and can perform a variety of specialized tasks that are impossible for other robots to do. The cost of such versatility is having to coordinate the many degrees of freedom these robots need to effectively emulate their biological counterparts. In previous work, the *serpenoid curve* was developed to seamlessly coordinate the many degrees of freedom in order to produce the desired behavior [1, 2]. In our previous work, we extended the planar version of the serpenoid curve into three dimensions, creating what we refer to as the *compound serpenoid curve* [3, 4, 5], which makes it possible to model biologically inspired snake-like motions, such as sidewinding, which have in-plane as well as out-of-plane motion. This is an advance over the traditional serpenoid curve, which can only be used to model predominantly in-plane motions like slithering.

While the serpenoid curve and compound serpenoid curve models have existed in the robotics community for some time, a very similar concept, known as a control template, has co-existed within the biological locomotion community. In the biological literature, a control template is defined in terms of a model of a behavior that "contains the smallest number of variables and parameters that exhibits a behavior of interest" [6, 7, 8]. Control templates thus make it possible to use low-dimensional models to represent and subsequently study various aspects of biological motion control [9, 10, 11]. So far, however, the template model in biology has mostly been restricted to planar locomotion and thus is not sufficient to capture a large subset of biological locomotor modes.

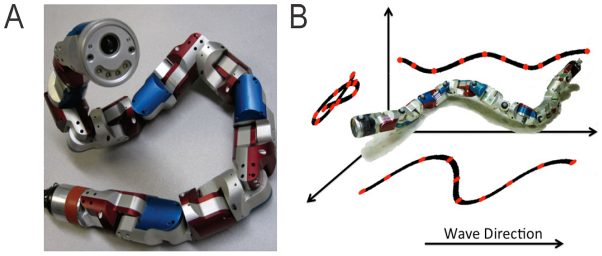

Fig. 1. (A) A 16-joint modular snake robot. (B) Two independent orthogonal serpenoid waves propagating down the snake's body while sidewinding.

In this work, we propose to extend the compound serpenoid curve for modular snake robots to biological control templates into three dimensions, which we refer to as the *compound-wave control template*. The purpose of this extension is twofold. First, we wish to provide a means for biologists to better model and examine the three-dimensional behaviors exhibited by limbless locomotion systems, e.g., sidewinding snakes. Second, biological intuition from control templates provides us with heuristics for low-dimensional motion design for snake robots, enhancing pre-existing capabilities as well as designing entirely new behaviors.

We first review the compound serpenoid wave control method. We then use the compound serpenoid curve as the basis for a new control template. On the biological side, we use this template to model two different turning behaviors observed in snakes. We then validate our models of applying the compound wave control templates to biological systems on a snake robot, using the parameters from the control template in the compound serpenoid model to generate the joint trajectories necessary to replicate the biological turning behavior. Subsequently, using the intuition gained by studying biological motion, we use a guided manual search of the compound-wave parameter space to derive a new turning motion which does not have a known biological counterpart nor has previously been demonstrated on a snake robot [12, 13].

Finally, to better understand the relationship between the compound-wave control methods and resultant workspace displacements, we extract contact patterns for the various gaits studied in this paper using a simulated snake robot.

[1]J. Dai, T. Dear, M. Travers, C. Gong and H. Choset are with the Robotics Institute at Carnegie Mellon University, Pittsburgh, PA 15213, USA. {jind@, mtravers@andrew., tonydear@, chaohuig@, choset@}cmu.edu

[2]H. C. Astley and D. I Goldman are with the School of Physics, Georgia Institute of Technology, Atlanta, GA 30332, USA. {henry.astley, daniel.goldman}@physics.gatech.edu

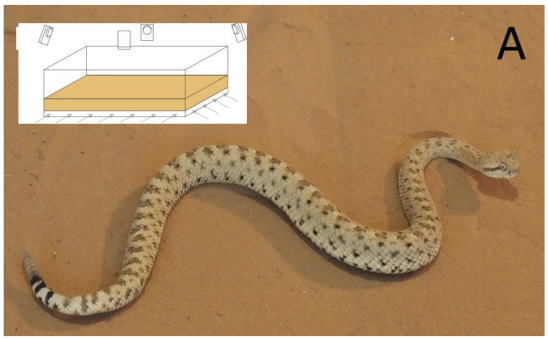

Fig. 2. A sidewinder rattlesnake (*Crotalus cerastes*) performs sidewinding locomotion on sand. Inset: a 1 m by 2 m fluidized bed trackway filled with sand.

This allows us to begin exploring the relationship between the coordination of the dorsal wave in the compound wave model and the resultant contact the snake's body makes with the environment.

II. COMPOUND SERPENOID CURVE

In his pioneering work on snake locomotion, Hirose proposed that the planar slithering motion of biological snakes could be represented using a serpenoid curve, a curve with sinusoidally varying curvature [1]. However, as we note in our previous work, this planar model cannot sufficiently capture many of the observed locomotion patterns in biological snakes. This limitation is mainly due to the ability of biological snakes to directly manipulate their contact with the surrounding environment by lifting and lowering portions of their bodies [14].

The compound serpenoid curve proposed in our previous work partially addresses this limitation. This model includes two separate sinusoidal expressions for the horizontal and vertical waves, giving the joint angle α at a particular joint index n and time t for each case.

$$\begin{aligned} \alpha(n,t) &= \begin{cases} \beta_h + A_h(n)\sin(\theta_h) & \text{horizontal} \\ \beta_v + eA_v(n)\sin(\theta_v + \delta) & \text{vertical} \end{cases} \\ \theta_{h,v}(n,t) &= \Omega_{h,v}n + \omega_{h,v}t \end{aligned} \quad (1)$$

where β, A, θ, e, δ, Ω, and ω are angle offset, amplitude, phase, aspect ratio, phase shift, spatial frequency, and temporal frequency, respectively.

The ten parameters in Eqn. (1) can be used to coordinate an arbitrary number of joints for a snake robot such as one with the configuration shown in Fig. 1B. This model has previously been shown to produce a variety of locomotive modes [3, 4, 5, 12, 13].

III. FROM ROBOTICS TO BIOLOGY

A. Snake Sidewinding Behavior

Biologists define a *template* as a simple model of a behavior, often with a low number of parameters, that can model the complex locomotion of organisms. For snakes and other multi-joint undulatory systems, the serpenoid curve naturally plays the role of such a template. Traditionally, however, this equivalence has been restricted to modeling planar locomotion and has not been extended to behaviors with out-of-plane motion, such as sidewinding.

Turn characteristics	Mean turn angle
Differential turning (per gait cycle)	$26.3° \pm 18.3°$
Reversal turning (in total)	$89.4° \pm 28.2°$

TABLE I
MEASUREMENTS FROM BIOLOGICAL SIDEWINDER OBSERVATIONS

In this section we present observations of biological snake sidewinding and show that the interplay between planar and non-planar components of the motion can be modeled with two independent orthogonal serpenoid waves propagating down the snake's body. We therefore propose a more generalized template, which we term the *compound wave template*. This template can be thought of as a direct extension of the compound-serpenoid curve prescribed in Section II. Using this template, we show that we are able to parameterize several biological snake motions which previously have not been modeled nor well understood.

B. Sidewinding Turning Modes

Sidewinder rattlesnakes (*Crotalus cerastes*) use at least two discrete turning mechanisms to change direction, which we term "differential turning" and "reversal turning." Measurements taken from overhead video capture of the snake are shown in Table I. Differential turns have a shallower turning angle θ_d but can continue for many cycles (Fig. 3C), while reversal turns are sharp and sudden with a large turning angle θ_r (Fig. 3E). We note that the high variance values indicate not measurement error, but rather the behavioral versatility typical of freely behaving animals—by varying their behavior, the snakes can achieve a huge range of turn angles.

1) Differential Turning: During differential turns, body segments furthest from the center of rotation cover a greater distance than body segments closest to the center of rotation, labeled as d_1 and d_2, respectively, in Fig. 3C. Considering the undulatory nature of snake locomotion, we can view the execution of this asymmetric motion as forcing the further end to undulate with a larger amplitude than the closer end. Thus, we model differential turning by imposing an amplitude gradient in the horizontal wave along the body. For example, a simple gradient can be modeled using a linear function in the horizontal wave amplitude along the snake's body, as shown in the second row of Table II. This choice was validated by a further observation that the difference $|d_1 - d_2|$ was proportional to the change in direction in biological snakes, indicating a direct relation between the amplitude gradient and the rate of turning (net change of orientation per gait cycle) [15]. This model also encompasses straight-line sidewinding as a special case, wherein amplitude is constant along the body ($k = 0$) and $|d_1 - d_2| \approx 0$. Finally, the vertical wave amplitude remains unchanged; Fig. 3D presents

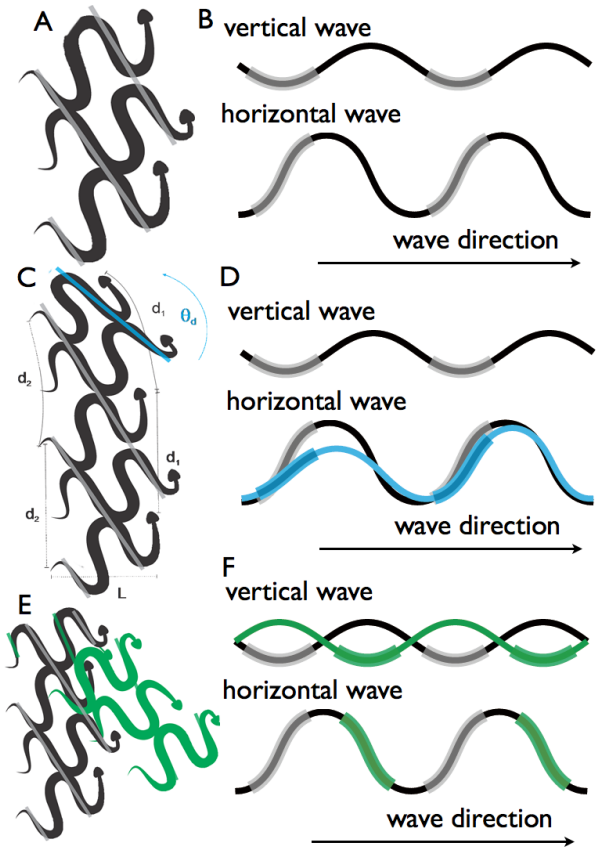

Fig. 3. (A) A diagram of typical sidewinding in a snake. Grey regions on the snake's body indicate ground contact, while other regions are lifted and moving. Tracks are shown in grey rectangles. (B) Horizontal and vertical body waves during straight-line sidewinding, offset by a phase difference $\phi = -\pi/2$. Grey regions indicate static contact. The arrow depicts the posterior propagation of waves down the body. (C) Straight-line sidewinding (grey) followed by differential turning (blue), with the snake turning upward at θ_d degrees. The distance moved is d_1 for the head and d_2 for the tail. (D) Horizontal and vertical waves of the robot during normal sidewinding (black) and differential sidewinding (blue). (E) Straight-line sidewinding (grey) followed by reversal turning (green), with the snake turning downward at θ_r. Relative to the direction of motion, the head is initially to the right of the body, but is on the left after the reversal. (F) Horizontal and vertical waves of the robot during normal sidewinding (black) and immediately following reversal turning (green).

a graphical representation of these waves.

2) Reversal Turning: Like differential turns, reversal turns also produce a change in the direction of travel, but we found that the mechanism by which this is achieved is significantly different. Sharp turns, some up to 160°, were observed, but all without apparent body rotation. Before and after the reversal run, there is no noticeable change of undulation in the horizontal plane. Instead, we noticed that the positions at which the snakes made contact with the environment switched very abruptly. In Fig. 3E, the grey and green segments of the snake's body are those in contact with the ground before and after the turn, respectively. At the time of the reversal turning (topmost snapshot), body segments in static contact with the ground instantaneously switch roles with segments in the air.

Because this change occurs in the vertical direction, we

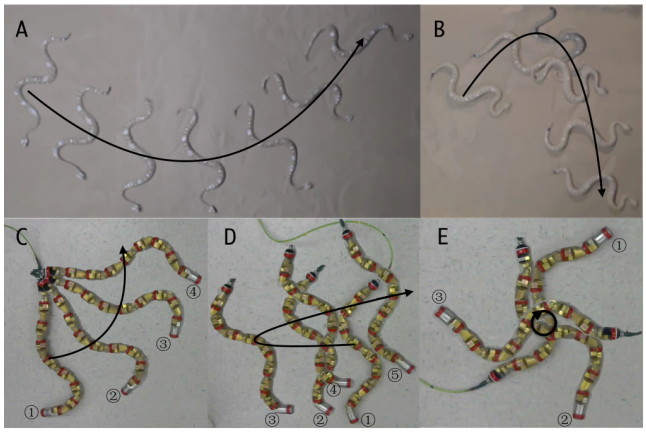

Fig. 4. (A) Differential and (B) reversal turning in a sidewinder rattlesnake. (C) Differential (parameters $k = 0.08$, $b = 0$) and (D) reversal turning implemented on a snake robot. (E) Demonstration of frequency turning.

Mode of Locomotion	$A_h(n)$	δ
Straight-line Sidewinding	Constant	$\frac{\pi}{2}$
Differential Turning	$kn + b$	$\frac{\pi}{2} \Rightarrow \frac{\pi}{2}$
Reversal Turning	Constant	$\frac{\pi}{2} \Rightarrow \frac{3\pi}{2}$

TABLE II
PARAMETERS FOR COMPOUND SERPENOID CURVE

propose that this transition can be modeled by adding a π radian phase offset to the vertical wave. We use a default phase shift of $\delta = \frac{\pi}{2}$, so it would change to $\frac{3\pi}{2}$, as shown in the last row of Table II. This flips the peak and valley points of the vertical wave, as illustrated in Fig. 3F, emulating the vertical body motion observed in the reversal turn. We hence parameterize reversal turns by adding a phase offset of π radians to the vertical component wave template. In contrast to differential turning, the amplitudes of the waves are constant, and all of the other horizontal and vertical wave parameters are held constant.

While these behaviors would have been impossible to emulate with the old serpenoid curve model, our proposed compound wave template easily accommodates these changes. Differential turning occurs when the horizontal wave amplitude is varied while propagating along the body; this is reminiscent of a previously developed robot conical turning mechanism but lacking vertical amplitude modulation [5]. Reversal turning is modeled as a π radian phase shift in the vertical wave, switching the roles of the contact and elevated segments but not affecting the propagation of the horizontal wave.

IV. EXPERIMENTAL VALIDATION

The compound wave template is a valuable tool for studying biological locomotion, but we would like to take this investigation one step further: experimentally validating

Turn characteristics	Mean turn angle
Differential turning (per gait cycle)	$30.1^\circ \pm 4.4^\circ$
Reversal turning (in total)	$127.2^\circ \pm 13.1^\circ$

TABLE III

DATA FROM EXPERIMENTS ON SNAKE ROBOT

our observations using a modular snake robot. We emphasize that we seek only to reproduce the qualitative behavior of the biological snakes, not necessarily the quantitative observed values, due to the differences in morphology between the robot and snake. In particular, the data in Table I show high variance, which again is a statistical statement of biological behavior. The scope of our experiments here is to reproduce not this versatility, but rather the behaviors in general. We thus refer to previous studies in [4], which showed that we can tune the slope of horizontal wave to achieve a desired turning angle with small variance. To experimentally achieve the same biological variance would likely require sweeping the other parameters not specified in Table I.

For our experiments, we placed the snake robot on hard ground and attached red tracking markers uniformly along the body. Both types of turning maneuvers were attempted for ten trials each. We commanded five integral gait cycles for each trial and measured the change of snake robot orientation based on the tracking information from the overhead camera; snapshots are shown in Fig. 4. For differential turning, we used the following gait equation with a linearly varying amplitude in the horizontal wave.

$$\alpha(n,t) = \begin{cases} 0.08n \times \sin(\frac{2\pi n}{12} - t) & n \text{ is odd} \\ 0.3\sin(\frac{2\pi n}{12} - t + \frac{\pi}{2}) & n \text{ is even} \end{cases} \quad (2)$$

For reversal turning, we used the gait equation

$$\alpha(n,t) = \begin{cases} 1.0\sin(\frac{2\pi n}{12} - t) & n \text{ is odd} \\ 0.3\sin(\frac{2\pi n}{12} - t + \delta) & n \text{ is even} \end{cases} \quad (3)$$

where $\delta = \frac{\pi}{2}$ for $t < t_{\text{reversal}}$ and $\delta = \frac{3\pi}{2}$ for $t > t_{\text{reversal}}$ as indicated in Table II.

The turning angle data from these experiments are shown in Table III. Not only were both maneuvers executed successfully, but the turning trials were qualitatively similar to those executed by the rattlesnake (Fig. 4A,B), whereby differential turning is achieved by varying the distance traveled by the two ends of the robot, and reversal turning is achieved by switching the velocity direction (Fig. 4C,D). In both cases, the similarity is within the scope of the variation allowed by the biological template, representing quantitative variations of the modifications of the template which allow turning.

We then used the biological parameters as a heuristic to further explore the parameter space of the compound wave template. This allows us to expand beyond what is currently known about biological systems, highlighting the power of template-based locomotion control. Our approach used the relative modulation of parameters between the two waves

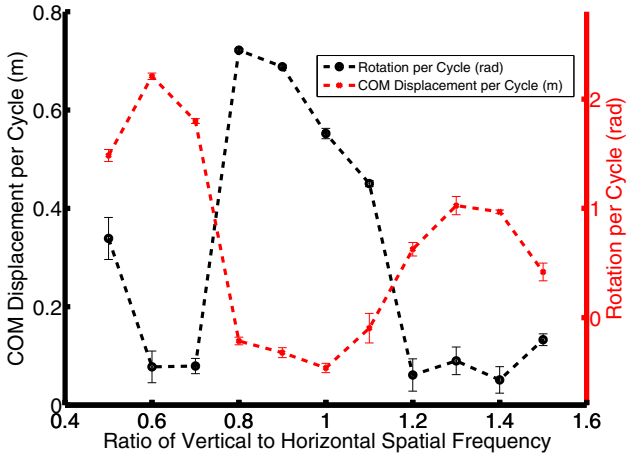

Fig. 5. Displacement of center of mass and turning rate with respect to vertical spatial frequency (relative to horizontal frequency).

in the template as the basis for exploration. While many parameter combinations were either deleterious or neutral, certain combinations of vertical to horizontal wave frequency ratios produced a turning behavior not seen in the biological snakes, which we term "frequency turning" (Fig. 4E).

To produce this technique, we systematically changed the ratio of vertical to horizontal spatial frequency, and measured the rotation per cycle and displacement of center of mass per gait cycle as shown in Fig. 5. The optimal frequency ratio for greatest rotation per cycle was achieved by setting $\Omega_v = 0.6\Omega_h$, while leaving all the rest of the parameters identical to that of straight-line sidewinding:

$$\alpha(n,t) = \begin{cases} 1.0\sin(\frac{2\pi n}{12} - t) & n \text{ is odd} \\ 0.3\sin(0.6 \times \frac{2\pi n}{12} - t + \frac{\pi}{2}) & n \text{ is even} \end{cases} \quad (4)$$

At this frequency ratio, forward displacement per cycle declined sharply while the robot rotated at up to 127° per cycle with small turning radius (Fig. 5). Further experiments on sand in [15] showed that this novel turn-in-place gait is robust enough to be reliably achieved on granular terrain with the same gait parameters. We hypothesize that this motion can be attributed mainly to the pattern of ground contact regions along the horizontal wave, which we explore in the following section.

V. A DEEPER INVESTIGATION OF VERTICAL WAVE

None of the turning techniques introduced in this paper have previously been modeled by biologists. We have shown that we are able to derive parameterized models for each of these locomotive modes using the compound wave template. This highlights the importance of vertical waves in modeling the rich set of three-dimensional motions which biological snakes exhibit. Upon further analysis, we have observed that even for the same horizontal wave patterns, differences in the vertical waves can result in distinct motions. This has triggered our interest to further investigate how the vertical waves distinctly affect net motion.

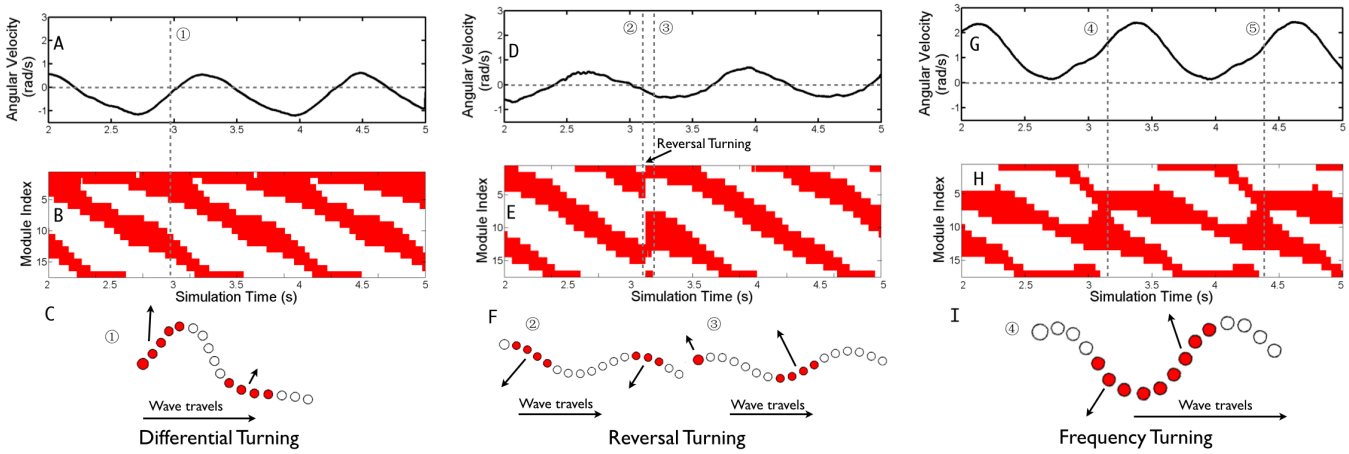

Fig. 6. Contact Pattern Analysis: the upper charts A, D, and G show the cyclic development of rotation velocity of the whole body, rather than CoM direction change, of differential turning, reversal turning and frequency turning; the lower graphs B, E, and H represent the contact patterns over time. Red blocks indicate contact of the indexed modules at that time point. Snapshots of the robot configuration and schematic forces for selected modules are shown for each motion in C, F, and I. The contact modules are also shown in red.

Our goal in this section is to examine the contact patterns associated with the different behaviors discussed in this work. Because of the unavailability of tactile sensing on our snake robot, we used a dynamic simulator to extract the contact patterns for a simulated modular snake robot. The fidelity of the dynamic simulator was validated by comparing the simulated snake motions with the actual robot motions.

A. Differential Turning

Differential turning was generated using the gait equation of Eqn. (2). In simulation, the snake's center of mass moved along a circular path with angular velocity of nonzero mean, measured in terms of an average body frame located at the COM and aligned with the average link orientation.

As shown in Fig. 6B, the contacts of differential turning showed a clear pattern: the snake had two or three contact segments with the ground at every time step and the positions of the contacts shifted from the head to tail at an constant speed. This contact pattern matches the description of sidewinding in biological literature [16]. The ground reaction forces experienced at the points of contacts were roughly parallel to each other but of different magnitudes. The difference in the magnitude resulted in a net torque that slowly drove the snake to rotate.

B. Reversal Turning

Reversal turning was simulated via the gait equation (3). Before and after the reversal, the contact pattern shown in Fig. 6E is similar to straight-line sidewinding. However, at the moment of reversal, the positions of contacts along the body changed abruptly. The lifted and grounded body segments switched their roles, resulting in ground reaction forces pointing in a reversed direction.

C. Frequency Turning

Frequency turning was readily achieved by setting $\Omega_v = 0.6\Omega_h$, while leaving all the rest of the parameters identical to that of straight-line sidewinding (Eqn. (4)). In simulation, the snake reoriented about 120 degrees per gait cycle with an angular velocity varying between 0 and 2.3 rad/s, measured in terms of rotation of the average body frame.

The contact pattern of frequency turning, as shown in Fig. 6H, is qualitatively different from that of straight-line sidewinding. We observed that at the times that the snake reaches high angular velocity, labeled as 4 and 5 in Fig. 6G, the middle segment of the snake forms a continuous region of contact with the ground. Fig. 6I shows that the contact modules on opposite sides of the wave peak experience ground reaction forces pointing in different directions. These forces effectively produced a net torque that drove the snake to rotate.

D. Discussion

Unlike the horizontal waves, vertical waves control contact, but don't generate propulsive force on their own. The qualitatively different contact patterns associated with the different turning modes explicitly showed how the modulation in the vertical wave changed the way the snake interacts with the ground and hence resulted in completely different behaviors. The horizontal wave coupled with the vertical wave together determine the positions and directions of the ground reaction forces and these forces determine the resultant motion. Better understanding of how the horizontal and vertical waves interact with the environment to impact the snake motion is an important step toward devising gaits that could ultimately overcome unstructured environments.

VI. CONCLUSIONS

A variety of motions, including straight-line sidewinding, reversal turning, differential turning, and frequency turning all emerged from the compound wave control template, showing the generality of this framework. The benefit of the compound wave control template is its readiness in controlling the motions by simply regulating a few parameters,

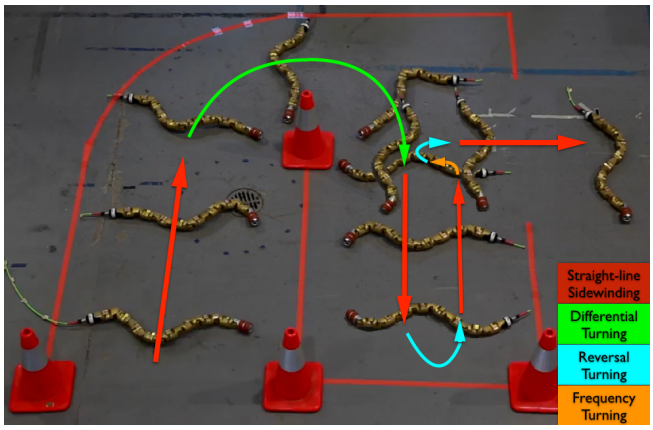

Fig. 7. Images from a video showing the sidewinder robot moving through a complex trackway using three turn types and straight-line sidewinding. Human operator control is simplified to four buttons, one for each type of motion. When following a gently curved path, the operator used a joystick to regulate the amplitude gradient of different turning to keep the robot along the track. Reversal turning was utilized when the robot hit a dead end and frequency turning was used to quickly reorient the robot.

which reduces control of a high degree of freedom robot to a manageable level for a human operator. We would like to conclude our discussion with a robot demonstration to highlight the benefits of controlling a snake robot using the compound wave control template. Fig. 7 shows a test course, which requires non-trivial maneuvers for successful traversal. In the test, a user was asked to use a game controller, with buttons mapped to the wave parameters in the compound wave template, to steer the snake robot along the course. Because of the conciseness of the compound wave control template, the operator was able to intuitively control the motion of the snake robot by simply pressing a button (transition between motions) or adjusting the joystick (regulating the amplitude gradient of differential turning).

In this work, we extended the biological notion of control template to three dimensions to produce a "compound wave template," to both better model biology as well as to endow snake robots with enhanced capabilities. Using this compound wave template, we were able to better explore the control space of a sidewinding snake and gain insight into how to modulate the vertical and horizontal wave parameters to produce interesting behaviors. In particular, we were able to replicate sidewinding, differential turning, and reversal turning observed in biological snakes on a snake robot by regulating few control inputs. Additionally, further exploration of the compound wave template parameter space produced frequency turning behavior, which does not have a known biological correspondence. Based on these different modes of locomotion with respective maneuverability and simple controllability, we were then able to demonstrate a novel driving experience on the modular snake robot.

References

[1] S. Hirose, *Biologically Inspired Robots (Snake-like Locomotor and Manipulator)*. Oxford University Press, 1993.

[2] M. Saito, M. Fukaya, and T. Iwasaki, "Modeling, analysis, and synthesis of serpentine locomotion with a multilink robotic snake," *IEEE Control Systems Magazine*, vol. 22, no. 1, pp. 64–81, 2002.

[3] M. Tesch, K. Lipkin, I. Brown, R. Hatton, A. Peck, J. Rembisz, and H. Choset, "Parameterized and scripted gaits for modular snake robots," *Advanced Robotics*, vol. 23, no. 9, pp. 1131–1158, 2009.

[4] C. Gong, M. J. Travers, X. Fu, and H. Choset, "Extended gait equation for sidewinding," in *Robotics and Automation (ICRA), 2013 IEEE International Conference on*. IEEE, 2013, pp. 5162–5167.

[5] C. Gong, R. L. Hatton, and H. Choset, "Conical sidewinding," *Robotics and Automation (ICRA)*, 2012.

[6] M. H. Raibert, *Legged robots that balance*. MIT press, 1986.

[7] P. Holmes, R. J. Full, D. Koditschek, and J. Guckenheimer, "The dynamics of legged locomotion: Models, analyses, and challenges," *Siam Review*, vol. 48, no. 2, pp. 207–304, 2006.

[8] J. Schmitt, M. Garcia, R. Razo, P. Holmes, and R. J. Full, "Dynamics and stability of legged locomotion in the horizontal plane: a test case using insects," *Biological cybernetics*, vol. 86, no. 5, pp. 343–353, 2002.

[9] H. Marvi, C. Gong, N. Gravish, H. Astley, M. Travers, R. L. Hatton, J. R. Mendelson, H. Choset, D. L. Hu, and D. I. Goldman, "Sidewinding with minimal slip: Snake and robot ascent of sandy slopes," *Science*, vol. 346, no. 6206, pp. 224–229, 2014.

[10] R. J. Full and D. E. Koditschek, "Templates and anchors: neuromechanical hypotheses of legged locomotion on land," *Journal of Experimental Biology*, vol. 202, pp. 3325–3332, 1999.

[11] D. I. Goldman, T. S. Chen, D. M. Dudek, and R. J. Full, "Dynamics of rapid vertical climbing in cockroaches reveals a template," *Journal of Experimental Biology*, vol. 209, no. 15, pp. 2990–3000, 2006.

[12] K. Melo and L. Paez, "Experimental determination of control parameter intervals for repeatable gaits in modular snake robots," in *Safety, Security, and Rescue Robotics (SSRR), 2014 IEEE International Symposium on*. IEEE, 2014, pp. 1–7.

[13] J. Gonzalez-Gomez, H. Zhang, E. Boemo, and J. Zhang, "Locomotion capabilities of a modular robot with eight pitch-yaw-connecting modules," in *9th international conference on climbing and walking robots*, 2006.

[14] B. C. Jayne, "Kinematics of terrestrial snake locomotion," *Copeia*, pp. 915–927, 1986.

[15] H. C. Astley, C. Gong, J. Dai, M. Travers, M. M. Serrano, P. A. Vela, H. Choset, J. Mendelson III, D. L. Hu, and D. I. Goldman, "Modulation of orthogonal body waves enables high maneuverability in sidewinding locomotion," *Proceedings of the National Academy of Sciences, in press*, 2015.

[16] W. Mosauer, "A note on the sidewinding locomotion of snakes," *American Naturalist*, pp. 179–183, 1930.